

# Electrical and Dielectric Properties, and Accelerated Aging Characteristics of Lanthania Doped Zinc Oxide Varistors

Choon-Woo Nahm<sup>a</sup>

*Department of Electrical Engineering, Donggeui University,  
Gaya 3-dong, Busanjin-gu, Busan 614-714, Korea*

<sup>a</sup>E-mail : [cwnahm@deu.ac.kr](mailto:cwnahm@deu.ac.kr)

(Received June 26 2006, Accepted July 28 2006)

The microstructure, electrical and dielectric properties, and stability against DC accelerated aging stress of the varistors, which are composed of quaternary system ZnO-Pr<sub>6</sub>O<sub>11</sub>-CoO-Cr<sub>2</sub>O<sub>3</sub>-based ceramics, were investigated for different La<sub>2</sub>O<sub>3</sub> contents. The increase of La<sub>2</sub>O<sub>3</sub> content led to more densified ceramics, whereas abruptly decreased the nonlinear properties by incorporating beyond 1.0 mol%. The highest nonlinearity was obtained from 0.5 mol% La<sub>2</sub>O<sub>3</sub>, with the nonlinear coefficient of 81.6 and the leakage current of 0.1  $\mu$ A. The varistors doped with 0.5 mol% La<sub>2</sub>O<sub>3</sub> exhibited high stability, in which the variation rates of breakdown voltage, nonlinear coefficient, leakage current, dielectric constant, and dissipation factor were -1.1 %, -3.7 %, +100 %, +1.4 %, and +8.2 %, respectively, for stressing state of 0.95 V<sub>1 mA</sub>/150 °C/24 h.

**Keywords :** Microstructure, Pr<sub>6</sub>O<sub>11</sub>, La<sub>2</sub>O<sub>3</sub>, Electrical properties, Varistors, Stability

## 1. INTRODUCTION

ZnO is oxide-semiconductor of non-stoichiometric defect structure that the zinc ion is more than oxygen ion. Therefore, ZnO is usefully used as material applying to gas sensor, devices using grain boundary effect, and so on. ZnO varistors are solid-state electronic devices manufactured by sintering a semiconducting ZnO powder with minor additives, such as Bi<sub>2</sub>O<sub>3</sub>, Pr<sub>6</sub>O<sub>11</sub>, CoO, Cr<sub>2</sub>O<sub>3</sub>, and so on. ZnO varistors exhibit highly nonlinear conduction characteristics. In other words, ZnO varistors act as an insulator below the breakdown voltage and a conductor thereafter. Moreover, ZnO varistors possess excellent surge withstanding capability. Therefore, they have been widely applied to surge protection device (SPD) such as the surge absorbers in electronic systems and the surge arresters in electric power systems[1,2].

Their electrical characteristics are related to a unit structure composed of ZnO grain-intergranular layer-ZnO grain in the bulk of the devices. A unit structure acts as if it is has a semiconductor junction at grain boundary. Since the nonlinear electrical behavior occurs at a boundary of each semiconducting ZnO grain, the varistors can be considered a multi-junction device

composed of many series and parallel connection of grain boundary. The grain size distribution plays a major rule in electrical behavior.

Many researchers who are interested in the varistors commonly wish to fabricate the ZnO varistors having a higher nonlinearity. The majority of commercial varistors are ZnO-Bi<sub>2</sub>O<sub>3</sub>-based varistors containing Bi<sub>2</sub>O<sub>3</sub>, which inherently induces nonlinear properties. Recently, ZnO-Pr<sub>6</sub>O<sub>11</sub>-based varistors are actively being studied in order to improve a few drawbacks[3] due to the high volatility and reactivity of Bi<sub>2</sub>O<sub>3</sub>[4-12]. Nahm et al. reported that ZnO-Pr<sub>6</sub>O<sub>11</sub>-based varistors have high nonlinear properties and high resistance against Dc accelerated aging stress by incorporating of rare-earth metal oxides[7-12].

This paper is to investigate the influence of lanthania (La<sub>2</sub>O<sub>3</sub>) on microstructure, electrical and dielectric properties, and stability of quaternary system ZnO-Pr<sub>6</sub>O<sub>11</sub>-CoO-Cr<sub>2</sub>O<sub>3</sub>-based varistors.

## 2. EXPERIMENTAL PROCEDURE

### 2.1 Sample preparation

Reagent-grade raw materials were prepared for ZnO varistors with composition (98.5-x) mol% ZnO+0.5

mol%  $\text{Pr}_6\text{O}_{11}$ +0.5 mol%  $\text{CoO}$ +0.5 mol%  $\text{Cr}_2\text{O}_3$ +x mol%  $\text{La}_2\text{O}_3$  (x = 0.0, 0.5, 1.0, 2.0). Raw materials were mixed by ball milling with zirconia balls and acetone in a polypropylene bottle for 24 h. The mixture was dried at 120 °C for 12 h and calcined in air at 750 °C for 2 h. The calcined mixture was pulverized using an agate mortar/pestle and after 2 wt% polyvinyl alcohol (PVA) binder addition, granulated by sieving 200-mesh screen to produce starting powder. The powder was uniaxially pressed into discs of 10 mm in diameter and 2 mm in thickness at a pressure of 80 MPa. The discs were covered with raw powder in alumina crucible, sintered at 1300 °C for 1 h. The sintered samples were lapped and polished to 1.0 mm thickness. The size of the final samples was about 8 mm in diameter and 1.0 mm in thickness. Silver paste was coated on both faces of samples and ohmic contact of electrodes was formed by heating at 600 °C for 10 min. The electrodes were 5 mm in diameter.

## 2.2 Microstructure examination

The either surface of samples was lapped and ground with SiC paper and polished with  $\text{Al}_2\text{O}_3$  powders to a mirror-like surface. The polished samples were thermally etched at 1100 °C for 30 min. The surface microstructure was examined by a scanning electron microscope (SEM, Hitachi S2400, Japan). The average grain size (d) was determined by the lineal intercept method as follows

$$d = \frac{1.56L}{MN} \quad (1)$$

where L is the random line length on the micrograph, M is the magnification of the micrograph, and N is the number of the grain boundaries intercepted by lines[13]. The crystalline phases were identified by an X-ray diffractometry (XRD, Rigaku D/max 2100, Japan) with  $\text{CuK}_\alpha$  radiation. The sintered density ( $\rho$ ) of ceramics was measured by the Archimedes method.

## 2.3 Electrical measurement

The V-I characteristics of the varistors were measured using a high voltage source measure unit (Keithley 237). The breakdown voltage ( $V_{1 \text{ mA}}$ ) was measured at a current density of 1.0 mA/cm<sup>2</sup> and the leakage current ( $I_L$ ) was measured at 0.80  $V_{1 \text{ mA}}$ . In addition, the nonlinear coefficient ( $\alpha$ ) was determined from the following expression[14].

$$\alpha = \frac{\log J_2 - \log J_1}{\log E_2 - \log E_1} \quad (2)$$

where  $J_1 = 1.0 \text{ mA/cm}^2$ ,  $J_2 = 10 \text{ mA/cm}^2$ , and  $E_1$  and  $E_2$  are the electric fields corresponding to  $J_1$  and  $J_2$ , respectively.

## 2.4 DC accelerated aging measurement

The stability against DC accelerated aging stress was performed under the four continuous states;

- (i) 1st stress: 0.85  $V_{1 \text{ mA}}/115^\circ\text{C}/24 \text{ h}$ ,
- (ii) 2nd stress: 0.90  $V_{1 \text{ mA}}/120^\circ\text{C}/24 \text{ h}$ ,
- (iii) 3rd stress: 0.95  $V_{1 \text{ mA}}/125^\circ\text{C}/24 \text{ h}$ ,
- (iv) 4th stress: 0.95  $V_{1 \text{ mA}}/150^\circ\text{C}/24 \text{ h}$ .

Simultaneously, the leakage current during the stress time was monitored at intervals of 1 min by a high voltage source-measure unit (Keithley 237). The varistors stressed were applied to the electrical characteristics after storage at normal room temperature for 2 h. The degradation rate coefficient ( $K_T$ ) was calculated from the following equation[15],

$$I_L = I_{L0} + K_T t^{1/2} \quad (3)$$

where  $I_L$  is the leakage current at stress time (t) and  $I_{L0}$  is  $I_L$  at t = 0. After the respective stresses, the V-I and dielectric characteristics were measured at room temperature. In treatment of numerical data, 5 sample varistors sintered at the same composition were used in all electrical measurements and their average value was used.

## 3. RESULTS AND DISCUSSION

Figure 1 shows the SEM micrographs of varistor ceramics with various  $\text{La}_2\text{O}_3$  contents. It is well known that the microstructure of  $\text{ZnO-Pr}_6\text{O}_{11}$ -based varistors is consisted of only two phases[16]:  $\text{ZnO}$  grain (bulk phase) and intergranular layer (second phase). The intergranular layers in varistors were Pr- and La-rich phases by XRD analysis, as shown in Fig. 2. As can be seen in the Figure, three diffraction peaks were revealed in varistors, namely,  $\text{ZnO}$  grains, Pr oxides, and  $\text{La}_2\text{O}_3$  oxide. It was observed by SEM that as the  $\text{La}_2\text{O}_3$  content increased, the intergranular phase gradually more distributed at the grain boundaries and particularly the nodal points. It is believed that this is attributed to the segregation of La toward grain boundaries due to the difference of ionic radius. These microstructures are not greatly different with varistors doped with Er, Y, and Dy, as reported previously[7,9,11]. As the  $\text{La}_2\text{O}_3$  content increased, the density increased from 4.71 to 5.77 g/cm<sup>3</sup> up to 1.0 mol%, whereas the further addition did not affect density, which saturated at 5.77 g/cm<sup>3</sup>. The average grain size increased from 4.0 to 8.5  $\mu\text{m}$  with increasing  $\text{La}_2\text{O}_3$  content due to precipitation of  $\text{Pr}_6\text{O}_{11}$  and  $\text{La}_2\text{O}_3$  at grain boundaries. Though the increase of  $\text{La}_2\text{O}_3$  content increased  $\text{La}_2\text{O}_3$  segregation at the grain boundaries, the average grain size increased with increasing  $\text{La}_2\text{O}_3$  content. In the light of increasing of

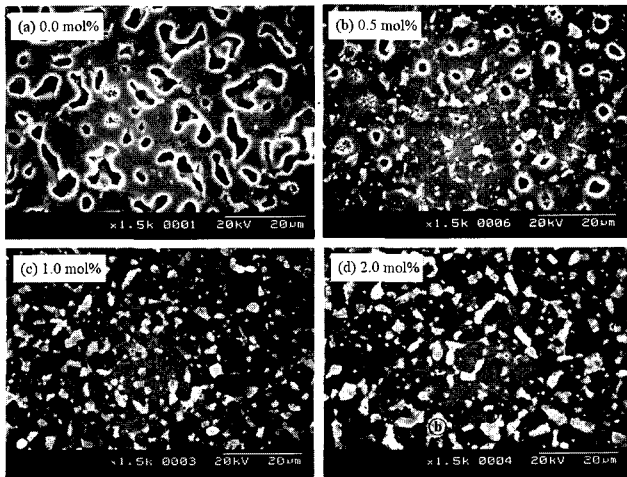


Fig. 1. SEM micrographs of varistors with various  $\text{La}_2\text{O}_3$  contents; (a) 0.0 mol%, (b) 0.5 mol%, (c) 1.0 mol%, and (d) 2.0 mol% (A: ZnO grain and B: intergranular layer).

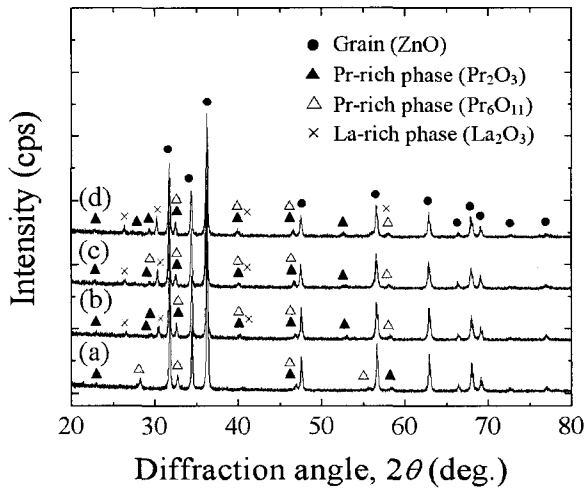


Fig. 2. XRD patterns of varistors with various  $\text{La}_2\text{O}_3$  contents; (a) 0.0 mol%, (b) 0.5 mol%, (c) 1.0 mol%, and (d) 2.0 mol%.

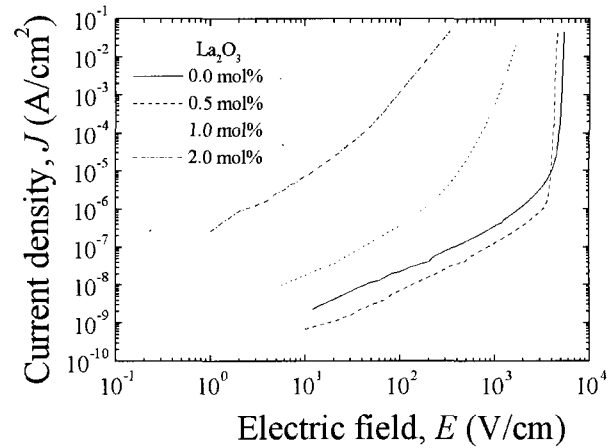


Fig. 3. E-J characteristics of varistors with various  $\text{La}_2\text{O}_3$  contents.

density and grain size for increasing  $\text{La}_2\text{O}_3$  segregation,  $\text{La}_2\text{O}_3$  seems to severe as an adder related to liquid phase sintering. The tendency of decrease in the average grain size directly affects the breakdown voltage in the electrical properties. The detailed microstructural parameters are summarized in Table 1.

Figure 3 shows the E-J characteristics of varistors with various  $\text{La}_2\text{O}_3$  contents. The conduction characteristics of varistors are divided into two regions: pre-breakdown at low field and breakdown at high field. The sharper the knee of the curves between the two regions, the better the nonlinearity. It can be forecasted that the varistors doped with 0.5 mol%  $\text{La}_2\text{O}_3$  would exhibit the best nonlinear properties because of the sharpest knee. Adding more  $\text{La}_2\text{O}_3$ , the knee gradually becomes less pronounced and the nonlinear properties reduce. The detailed V-I characteristic parameters are summarized in Table 1. The breakdown voltage ( $V_{1\text{mA}}$ ) decreased abruptly from 503.5 to 9.4 V/mm as the  $\text{La}_2\text{O}_3$  content increased. This is attributed firstly to the decrease in the number of grain boundaries caused by the increase in the ZnO grain size, and secondly, to the abrupt decrease of breakdown voltage

Table 1. Microstructure, V-I characteristic, and dielectric parameters of varistors with various  $\text{La}_2\text{O}_3$  contents.

$\text{La}_2\text{O}_3$ content (mol%)	$\rho$ ( $\text{g}/\text{cm}^3$ )	d ( $\mu\text{m}$ )	$V_{1\text{mA}}$ (V/mm)	$V_{\text{gb}}$ (V/gb)	$\alpha$	$I_{\text{L}}$ ( $\mu\text{A}$ )	$\epsilon_{\text{APP}}$ (1kHz)	$\tan\delta$ (1kHz)
0.0	4.71	4.0	503.5	2.0	63.0	2.1	484.7	0.0772
0.5	5.40	6.9	427.2	2.9	81.6	0.2	737.9	0.0784
1.0	5.77	7.9	108.0	0.8	7.1	50.6	2129.5	0.2839
2.0	5.77	8.5	9.4	0.08	3.1	100.2	2670.7	0.3885

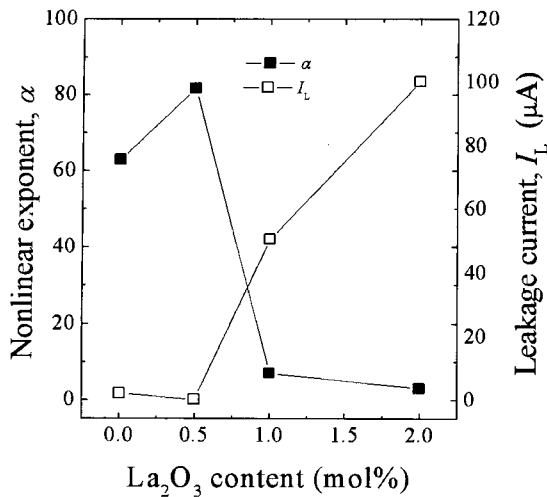


Fig. 4. Nonlinear coefficient and leakage current with various La<sub>2</sub>O<sub>3</sub> contents.

per grain boundaries ( $V_{gb}$ ). The varistors doped with La<sub>2</sub>O<sub>3</sub> exceeding 0.5 mol% exhibited much lower  $V_{gb}$  value than general value of 2-3 V/gb. These varistors will exhibit very poor nonlinear properties presumably. The breakdown voltage per grain boundaries ( $V_{gb}$ ) is defined by the following equation,

$$V_{gb} = \left(\frac{d}{D}\right)V_{1mA} \quad (4)$$

where  $d$  is the average grain size and  $D$  is thickness of sample.

The nonlinear coefficient ( $\alpha$ ) value was calculated to be 63.0 in the case of varistors without La<sub>2</sub>O<sub>3</sub>. This value was much higher than that of the quaternary system ZnO-Bi<sub>2</sub>O<sub>3</sub>-CoO-Cr<sub>2</sub>O<sub>3</sub>-based ceramics, which never exceed 25. As the La<sub>2</sub>O<sub>3</sub> content increased, the  $\alpha$  value increased, achieving a maximum value (81.6) for varistors with 0.5 mol% La<sub>2</sub>O<sub>3</sub>. This value is easily unobtainable excellent nonlinearity in ZnO varistors. This is the highest value in Pr<sub>6</sub>O<sub>11</sub>-based ZnO varistors of 5-components reported until now. Increasing La<sub>2</sub>O<sub>3</sub> content further to 2.0 mol% caused the  $\alpha$  value (3.1) to decrease. On the other hand, as the La<sub>2</sub>O<sub>3</sub> content increased, the leakage current ( $I_L$ ) value decreased, achieving a minimum value (0.2  $\mu$ A) for varistors with 0.5 mol% La<sub>2</sub>O<sub>3</sub>. Increasing La<sub>2</sub>O<sub>3</sub> content further to 2.0 mol% caused the  $I_L$  value (100.2  $\mu$ A) to increase extremely. It can be seen that the variation of  $I_L$  shows the inverse relationship to the variation of  $\alpha$  with La<sub>2</sub>O<sub>3</sub> content. As a result, it is clear that the nonlinear properties are strongly influenced by the incorporation of La<sub>2</sub>O<sub>3</sub>. It is confirmed that the reason why the varistors with 0.5 mol% La<sub>2</sub>O<sub>3</sub> exhibits highest nonlinearity is attributed to the highest barrier height at grain boundaries[17].

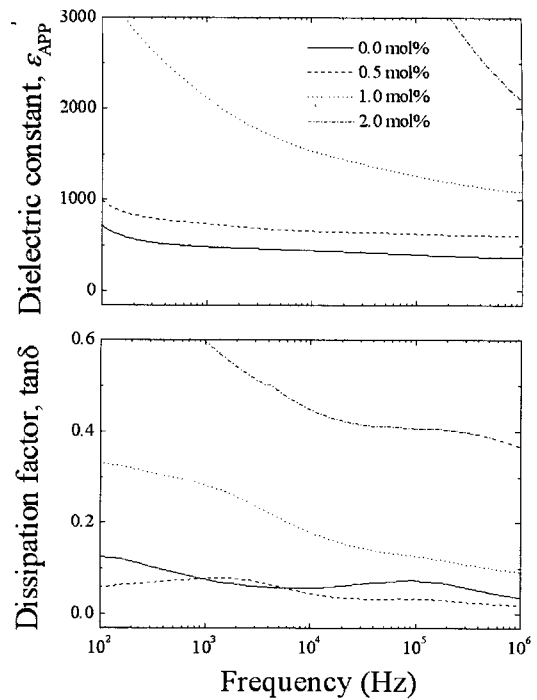


Fig. 5. Frequency dependence of dielectric characteristics of varistors with various La<sub>2</sub>O<sub>3</sub> contents.

Figure 5 shows the frequency dependence of dielectric characteristics of varistors with various La<sub>2</sub>O<sub>3</sub> contents. The apparent dielectric constant ( $\epsilon_{APP}$ ) decreased gradually without a sharper dispersive drop evident as the frequency increased, which is associated with the polarization of dielectrics. The apparent dielectric constant in the measuring frequency range increased with increasing La<sub>2</sub>O<sub>3</sub> content. This is directly related to the average grain size, as can be seen in the equation,

$$\epsilon_{APP} = \epsilon_g \frac{d}{t} \quad (5)$$

where  $\epsilon_g$  is the dielectric constant of ZnO,  $d$  is the average grain size, and  $t$  is the depletion layer width. It can be seen that the larger grain in comparison gives rise to a higher  $\epsilon_{APP}$  value. The detailed dielectric parameters at 1 kHz are summarized in Table 1. It was found that the values of dissipation factor ( $\tan\delta$ ) are very greatly affected by La<sub>2</sub>O<sub>3</sub> content and in gross, very complex. The  $\tan\delta$  of La<sub>2</sub>O<sub>3</sub> doped varistors except for varistors doped with 0.5 mol% La<sub>2</sub>O<sub>3</sub> exhibited to be very high more than 10 % at 1 kHz. Although the varistors with 0.5 mol% La<sub>2</sub>O<sub>3</sub> have low leakage current, the  $\tan\delta$  is high, compared with other rare-earth metal oxides like Er<sub>2</sub>O<sub>3</sub>, Y<sub>2</sub>O<sub>3</sub>, and Dy<sub>2</sub>O<sub>3</sub> less than 5 %. The  $\tan\delta$  is composed of joule heating loss by leakage current and friction heating

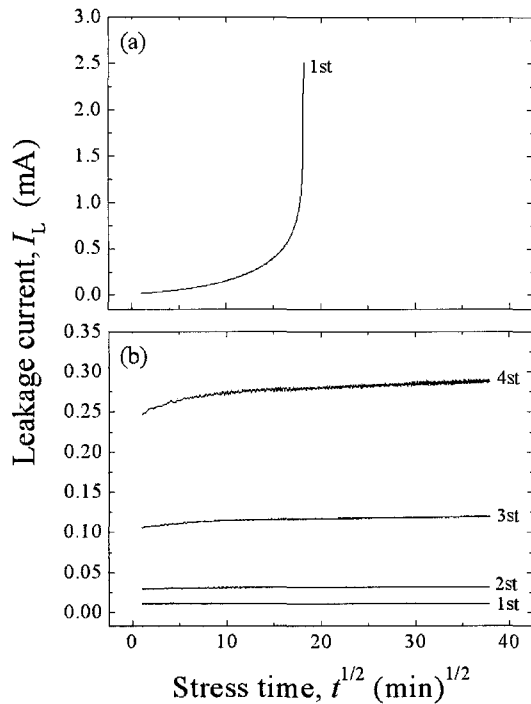


Fig. 6. Variation of leakage current during DC accelerated aging stress of varistors doped with  $\text{La}_2\text{O}_3$ ; (a) 0.0 mol% and (b) 0.5 mol%.

loss by electric dipole rotation. It is assumed that the reason why they exhibit high  $\tan\delta$  is because they are more greatly affected by the former than the latter.

Figure 6 shows the variation of leakage current during various DC accelerated aging stresses of varistors doped with 0.0 and 0.5 mol%  $\text{La}_2\text{O}_3$ , which have only high nonlinearity. The  $\text{ZnO-Pr}_6\text{O}_{11}\text{-CoO-Cr}_2\text{O}_3$ -based varistors doped without  $\text{La}_2\text{O}_3$  exhibited a thermal runaway under the first stress, even under relatively weak stress, exhibited the thermal runaway within short time. Although this varistor possesses a good nonlinearity, to be easily degraded is attributed to the low density, which decreases the number of conduction path and eventually leads to the concentration of current. On the other hand, the varistors doped with 0.5 mol%  $\text{La}_2\text{O}_3$  show high stability without thermal runaway until the 4th stress ( $0.95 V_{1\text{mA}}/150^\circ\text{C}/24\text{h}$ ). It can be seen that the leakage current was nearly constant ( $K_T = +0.24$  to  $0.25 \mu\text{A}\cdot\text{h}^{-1/2}$ ) until the 2nd stress ( $0.90 V_{1\text{mA}}/120^\circ\text{C}/24\text{h}$ ), but weak positive creep of leakage current ( $K_T = +1.48$  to  $1.50 \mu\text{A}\cdot\text{h}^{-1/2}$ ) under the 3rd stress ( $0.95 V_{1\text{mA}}/125^\circ\text{C}/24\text{h}$ ) and remarkable creep ( $K_T = +4.65$  to  $4.468 \mu\text{A}\cdot\text{h}^{-1/2}$ ) during the 4th stress ( $0.95 V_{1\text{mA}}/150^\circ\text{C}/24\text{h}$ ). It is assumed that this high stability is attributed to the density higher and the leakage current lower.

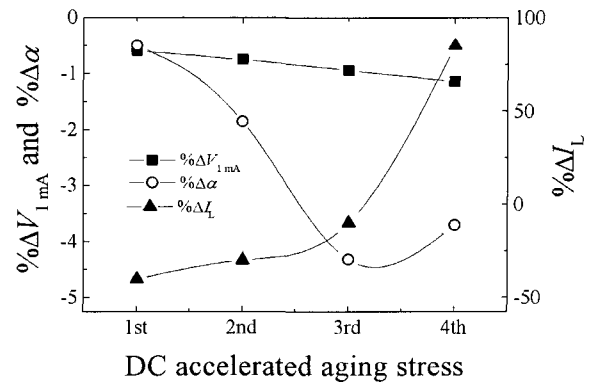


Fig. 7. Variation of breakdown voltage, nonlinear coefficient, and leakage current after DC accelerated aging stress of varistors doped with 0.5 mol%  $\text{La}_2\text{O}_3$ .

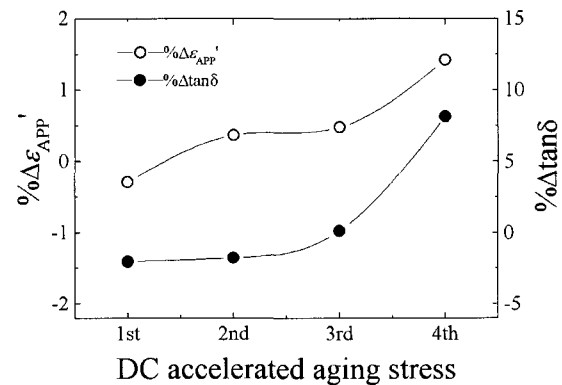


Fig. 8. Variation of apparent dielectric constant and dissipation factor after DC accelerated aging stress of varistors doped with 0.5 mol%  $\text{La}_2\text{O}_3$ .

Figure 7 shows the variation rates of the breakdown voltage ( $\% \Delta V_{1\text{mA}}$ ), variation rates of nonlinear coefficient ( $\% \Delta \alpha$ ), and variation rates of leakage current ( $\% \Delta I_L$ ) with various stresses in the varistors doped with 0.5 mol%  $\text{La}_2\text{O}_3$ . As the strength for stress severed, the  $V_{1\text{mA}}$  decreased, and  $\% \Delta \alpha$  and  $\% \Delta I_L$  increased.  $\% \Delta V_{1\text{mA}}$  exhibited much lower variation compared with  $\% \Delta \alpha$  and  $\% \Delta I_L$ . These varistors relatively exhibited high stability for V-I characteristics, in which  $\% \Delta V_{1\text{mA}}$  is  $-1.1\%$ ,  $\% \Delta \alpha$  is  $-3.7\%$ , and  $\% \Delta I_L$  is  $+100\%$  after the 4th stress. The leakage current greatly changed compared with initial value after the 4th stress, whereas only  $0.4 \mu\text{A}$ . On the other hand, the variation rate of dielectric constant ( $\% \Delta \epsilon_{\text{APP}}$ ) and variation rate of dissipation factor ( $\% \Delta \tan \delta$ ) with various stresses in the varistors doped with 0.5 mol%  $\text{La}_2\text{O}_3$  are shown in Fig. 8. Also the stability for dielectric characteristics exhibited a high stability, with  $\% \Delta \epsilon_{\text{APP}}$  of  $+1.4\%$  and  $\% \Delta \tan \delta$  of  $+8.2\%$ .

Table 2. Variation rate of V-I and dielectric parameters of after DC accelerated aging stress of varistors doped with 0.5 mol% La<sub>2</sub>O<sub>3</sub>.

Stress state	V <sub>1mA</sub> (V/mm)	%ΔV <sub>1mA</sub>	α	%Δα	I <sub>L</sub> (μA)	%ΔI <sub>L</sub>	ε <sub>APP'</sub>	%Δε <sub>APP'</sub>	tanδ	%Δtanδ
Before	427.2	0	81.6	0	0.2	0	737.9	0	0.0784	0
1st	424.7	-0.6	81.2	-0.5	0.1	-50	735.7	-0.3	0.0768	-2.0
2nd	424.0	-0.8	80.1	-1.8	0.1	-50	740.6	0.4	0.0770	-1.8
3rd	423.2	-0.9	78.1	-4.3	0.2	0	741.4	0.5	0.0785	0.1
4th	422.3	-1.1	78.6	-3.7	0.4	100	748.4	1.4	0.0848	8.2

The variations of V-I and dielectric parameters after various DC stresses in varistors doped with 0.5 mol% La<sub>2</sub>O<sub>3</sub> are summarized in Table 2.

#### 4. CONCLUSION

The microstructure, electrical and dielectric properties, and stability against DC accelerated aging stress of varistors were investigated with various La<sub>2</sub>O<sub>3</sub> contents. The sintered ceramics were more densified in the range of 4.71-5.77 g/cm<sup>3</sup> with increasing La<sub>2</sub>O<sub>3</sub> content. The breakdown voltage decreased abruptly in the range of 503.5 to 9.4 V/mm with increasing La<sub>2</sub>O<sub>3</sub> content. It was found that a moderate La<sub>2</sub>O<sub>3</sub> content, in the vicinity of 0.5 mol%, could greatly improve the nonlinear properties of quaternary system ZnO-Pr<sub>6</sub>O<sub>11</sub>-CoO-Cr<sub>2</sub>O<sub>3</sub>-based varistors. The varistors with 0.5 mol% La<sub>2</sub>O<sub>3</sub> exhibited excellent nonlinear properties, which the nonlinear coefficient is 81.6 and the leakage current is 0.2 μA. The La<sub>2</sub>O<sub>3</sub> seems to be additives acting as a donor by increasing the donor density with increasing La<sub>2</sub>O<sub>3</sub> content. The varistors doped with 0.5 mol% La<sub>2</sub>O<sub>3</sub> also exhibited high stability, with the variation rate of breakdown voltage of -1.1 %, of nonlinear coefficient of -3.7 %, of leakage current of +100 %, of dielectric constant of +1.4 %, and of dissipation factor of +8.2 % for stressing state of 0.95 V<sub>1mA</sub>/150 °C/24 h.

#### REFERENCE

- [1] L. M. Levinson and H. R. Philipp, "Zinc oxide varistor-a review", Amer. Ceram. Soc. Bull., Vol. 65, No. 4, p. 639, 1986.
- [2] T. K. Gupta, "Application of zinc oxide varistor", J. Amer. Ceram. Soc., Vol. 73, No. 7, p. 1817, 1990.
- [3] Y. S. Lee and T. Y. Tseng, "Phase identification and electrical properties in ZnO-glass varistors", J. Amer. Ceram. Soc., Vol. 75, No. 6, p. 1636, 1992.
- [4] A. B. Alles and V. L. Burdick, "The effect of liquid-phase sintering on the properties of Pr<sub>6</sub>O<sub>11</sub>-based ZnO varistors", J. Appl. Phys., Vol. 70, No. 11, p. 6883, 1991.
- [5] Alles, A. B., Puskas, R., Callahan, G., and Burdick, V. L., "Compositional effect on the liquid-phase sintering of praseodymium oxides-based ZnO varistors", J. Am. Ceram. Soc., Vol. 76, No. 8, p. 2098, 1993.
- [6] Y.-S. Lee, K.-S. Liao, and T.-Y. Tseng, "Microstructure and crystal phases of praseodymium in zinc oxides varistors", J. Amer. Ceram. Soc., Vol. 79, No. 9, p. 2379, 1996.
- [7] C.-W. Nahm, "The nonlinear properties and stability of ZnO-Pr<sub>6</sub>O<sub>11</sub>-CoO-Cr<sub>2</sub>O<sub>3</sub>-Er<sub>2</sub>O<sub>3</sub> ceramic varistors" Mater. Lett., Vol. 47, No. 4, p. 182, 2001.
- [8] C.-W. Nahm and J.-S. Ryu, "Influence of sintering temperature on varistor characteristics of ZPCCE-based ceramics", Mater. Lett., Vol. 53, No. 1-2, p. 110, 2002.
- [9] C.-W. Nahm, "Microstructure and electrical properties of Y<sub>2</sub>O<sub>3</sub> doped ZnO-Pr<sub>6</sub>O<sub>11</sub>-based varistor", Mater. Lett., Vol. 57, No. 7, p. 1317, 2003
- [10] C.-W. Nahm and B.-C. Shin, "Highly stable electrical properties of ZnO-Pr<sub>6</sub>O<sub>11</sub>-CoO-Cr<sub>2</sub>O<sub>3</sub>-Y<sub>2</sub>O<sub>3</sub>-based varistor ceramics", Mater. Lett., Vol. 57, No. 7, p. 1322, 2003.
- [11] C.-W. Nahm, "Microstructure and electrical properties of Dy<sub>2</sub>O<sub>3</sub>-based ZnO-Pr<sub>6</sub>O<sub>11</sub>-based varistor ceramics", Mater. Lett., Vol. 58, No. 17-18, p. 2252, 2004.
- [12] C.-W. Nahm and B.-C. Shin, "Effect of sintering time on electrical characteristics and DC accelerated aging behaviors of Zn-Pr-Co-Cr-Dy oxide-based varistors", J. Mater. Sci. Mater. Electron., Vol. 16, No. 11-12, p. 725, 2005.
- [13] J. C. Wurst and J. A. Nelson, "Lineal intercept tec-

- hnique for measuring grain size in two-phase polycrystalline ceramics", *J. Amer. Ceram. Soc.*, Vol. 55, No. 97-12, p. 109, 1972.
- [14] M. Matsuoka, "Nolinear properties of zinc oxide ceramics", *Jpn. J. Appl. Phys.*, Vol. 10, No. 9, p. 736, 1971.
- [15] J. Fan and R. Freer, "Deep level transient spectroscopy of zinc oxide varistors doped with aluminum oxide and/or silver oxide", *J. Amer. Ceram. Soc.*, Vol. 77, No. 10, p. 2663, 1994.
- [16] K. Mukae, "Zinc oxide varistors with praseodymium oxide", *Am. Ceram. Soc. Bull.*, Vol. 66, No. 9, p. 1329, 1987.
- [17] C.-W. Nahm, "Effect of  $\text{La}_2\text{O}_3$  addition on electrical characteristics of  $\text{Pr}_6\text{O}_{11}$ -based ZnO varistors", *Trans. EEM.*, Vol. 7, No. 3, p. 123, 2006.